Journal of Power Sources 251 (2014) 30–37

Contents lists available at ScienceDirect

Journal of Power Sources

journal homepage: www.elsevier.com/locate/jpowsour

The electrooxidation mechanism of formic acid on platinum and on lead ad-atoms modified platinum studied with the kinetic isotope effect

M. Bełtowska-Brzezinska [a,*], T. Łuczak [a], J. Stelmach [a], R. Holze [b]

[a] A. Mickiewicz University, Faculty of Chemistry, Grunwaldzka 6, 60-780 Poznań, Poland
[b] Technische Universität Chemnitz, Institut für Chemie, AG Elektrochemie, 09107 Chemnitz, Germany

HIGHLIGHTS

- Insight into mechanism of formic acid oxidation on Pt and Pt/Pb electrodes with kinetic isotope effect.
- Catalytic synergistic effect in direct oxidation of formic acid to CO_2 induced by upd-lead.
- Suppression of strongly bound CO-like species on upd-lead ad-atoms modified platinum electrode.
- The optimal conditions for monitoring of FA in acidic solution containing Pb^{2+} cations were specified.

ARTICLE INFO

Article history:
Received 26 July 2013
Received in revised form
18 October 2013
Accepted 9 November 2013
Available online 26 November 2013

Keywords:
Electrooxidation
Electrocatalysis
Fuel cell
Kinetic isotope effect
Formic acid

ABSTRACT

Kinetics and mechanism of formic acid (FA) oxidation on platinum and upd-lead ad-atoms modified platinum electrodes have been studied using unlabelled and deuterated compounds. Poisoning of the electrode surface by CO-like species was prevented by suppression of dissociative chemisorption of FA due to a fast competitive underpotential deposition of lead ad-atoms on the Pt surface from an acidic solution containing Pb^{2+} cations. Modification of the Pt electrode with upd lead induced a catalytic effect in the direct electrooxidation of physisorbed FA to CO_2. With increasing degree of H/D substitution, the rate of this reaction decreased in the order: HCOOH > DCOOH ≥ HCOOD > DCOOD. HCOOH was oxidized 8.5-times faster on a Pt/Pb electrode than DCOOD. This primary kinetic isotope effect proves that the C–H- and O–H-bonds are simultaneously cleaved in the rate determining step. A secondary kinetic isotope effect was found in the dissociative chemisorption of FA in the hydrogen adsorption–desorption range on a bare Pt electrode after H/D exchange in the C–H bond, wherein the influence of deuterium substitution in the O–H group was negligibly small. Thus the C–H bond cleavage is accompanied by the C–OH and not the O–H bond split in the FA decomposition, producing CO-like species on the Pt surface sites.

1. Introduction

An effective way to enhance the catalytic activity of noble metals (Pt, Pd, Au) in electrochemical reactions (in particular oxidations) of organic molecules and CO is their modification with a second metallic component with a different strength of adsorption of hydrogen and/or oxygen, realized by electro-deposition of foreign metals [1–18] or by alloying [12,19–23]. Recently, much attention has been paid to nanostructured mono-, bi- and multi-metallic systems [12,24–46] including core-shell-structured nanoparticles [47–50] or self assembled monolayers on electrodes [51–56]. These reported investigations have been mainly concerned with the influence of composition, support effects and other structural details on their efficiency as catalyst in fuel cells. However, despite of many reports, further extensive adsorption and kinetic studies are desired for better understanding of the mechanism of the catalytic reactions at such electrodes.

The purpose of this work is to present data on the kinetic isotope effect caused by systematic H/D substitution of formic acid (FA) as a useful way to gain deeper insight into the mechanism of the rate determining step (rds) in the electrooxidation of this compound on platinum and upd-lead ad-atoms modified platinum electrodes. Taking into account our earlier investigation dealing with the kinetics of formaldehyde adsorption and oxidation on Pt and Pt/Pb

* Corresponding author.
E-mail address: mbb@amu.edu.pl (M. Bełtowska-Brzezinska).

0378-7753/$ – see front matter © 2013 Elsevier B.V. All rights reserved.
http://dx.doi.org/10.1016/j.jpowsour.2013.11.027

electrodes in acidic medium [7], we now report results of experiments performed using cyclic voltammetry at moderate and fast sweep rates combined with chronoamperometry, aimed at further elucidation of the electrooxidation mechanism of FA at these electrodes.

2. Experimental

All measurements were performed at room temperature (298 K) in a conventional three compartment cell, separated by glass frits and equipped with a Luggin capillary at a distance of 2 mm from the working polycrystalline platinum (99.998%) sheet electrode of 1 cm^2 geometric area. A large area Pt sheet of the same purity was used as counter electrode. A hydrogen electrode filled with the supporting electrolyte solution (RHE) was used as reference [57]. Prior to each experiment, the working electrode was repeatedly activated in the deaerated supporting electrolyte solution by cycling (dE/dt = 5 V s^{-1}) in the potential range 0.025 V < E_{RHE} < 1.5 V until a reproducible voltammogram was obtained. Finally, the roughness factor of Pt (2.2 ± 0.2) was determined from the charge (Q_H = 0.46 mC cm^{-2}) corresponding to the hydrogen adsorption and/or desorption according to the well-known procedure [58], assuming that a hydrogen monolayer requires 0.21 mC cm^{-2}.

Cyclic voltammograms (CV) and chronoamperometric transients at E = const were obtained on a setup including a computer-controlled 9431 potentiostat (Atlas-Sollich, Poland) equipped with an IR-drop correction system coupled to a signal generator working in the triangular potential sweep mode with programmable potential sequences, potential ranges, number of cycles and scan rates as well as time periods with holding the electrode potential at a constant value. Current–potential–time dependencies were recorded and analysed with a computer-based system connected to a MC112-12 interface (Mescomp, Poland).

The following procedure was applied in the adsorption experiments. After a series of 8 potentiodynamic scans between 0.07 V and 1.65 V, the potential of the working electrode was held at E = 1.5 V for 5 ms and then switched (at dE/dt = 10 V s^{-1}) to different fixed E_{ad} values for various time periods, t_{ad}. Next, the species adsorbed on the Pt electrode were oxidized or reduced during the first positive or negative going potential sweep, respectively. The charge related to the electrooxidation of FA residues or upd-Pb ad-atoms (Q_{ox}) was determined by integration of the respective CVs recorded in the first and subsequent cycles. The coverage of the electrode surface with adsorbed species (θ) was evaluated from the difference (ΔQ_H) between the charge corresponding to the hydrogen desorption from Pt in the supporting electrolyte (Q_H^o) and after adsorption of FA (Q_H), according to the expression: $\theta = \Delta Q_H/Q_{ox} = (Q_H^o - Q_H)/Q_{ox}$. The rate of the electrode coverage was determined at various constant values of E_{ad} and different values of t_{ad} at constant values of $c_{Pb^{2+}}$ or c_{FA}. By comparing Q_{ox} with ΔQ_H, the number of electrons transferred per Pt site (n_{eps}) was calculated: $n_{eps} = Q_{ox}/\Delta Q_H$. It should be noted that the charge corresponding to the double layer or to the oxide layer formation in a supporting electrolyte solution was always subtracted from the total charge involved in the investigated electrode process. In chronoamperometric experiments the sequence of activating steps was followed by measurements of the current density–time (j–t) transients at constant electrode potentials, E_{ad}.

Electrolyte solutions were prepared using Millipore Milli-Q-water, HCOOH (p.a. LOBA, 99–100%), $HClO_4$ suprapur (Merck), $Pb(ClO_4)_2$ (SERVA, 50% sol.), DCOOD (p.a. MERCK, 100% D), DCOOH (99.85% D), p.a. $DClO_4$ and triply-distilled D_2O (IBJ Swierk, Poland). The concentrations of perchloric and formic acids were determined by titration. Argon 99.998% (BOC-Gas) was used for deaeration and stirring of the investigated solutions. $DClO_4$ was used in preparation of electrolyte solutions with D_2O and perdeuterated compounds.

3. Results and discussion

Representative CVs in Fig. 1, obtained at fast sweep conditions (dE/dt = 5 V s^{-1}) after holding the electrode potential within the hydrogen adsorption-desorption region, at E_{ad} = 0.2 V for t_{ad} = 180 s, illustrate differences in the catalytic properties of the Pt/Pb and Pt electrode in a supporting electrolyte solution (0.2 M $HClO_4$) containing 10^{-2} M HCOOH, with and without Pb^{2+} cations. Note, that the sweep rate chosen was high enough to determine the charge related to the oxidation of adsorbed species present at the electrode/solution interface only without any interference of Pb^{2+} and FA diffusing from the bulk of the solution to the electrode surface.

Strong poisoning of the Pt surface with irreversibly adsorbed species, formed of FA in the absence of Pb^{2+} cations in solution, is clearly indicated (trace 1 in Fig. 1) by suppression of the current related to the hydrogen electrosorption/desorption at $E \leq 0.4$ V and by the appearance of the anodic current peak between 0.75 V < E < 1.5 V corresponding to the oxidation of the adsorbate, with a maximum around 1 V. Evidently, the saturation coverage of Pt surface sites ($\theta \approx 1$) with the strongly bonded species is achieved under the above-mentioned experimental conditions (E_{ad} = 0.2 V, t_{ad} = 180 s). Accordingly, the platinum electrode is inactive for the oxidation of FA within the double layer potential range. The influence of FA concentration (c_{FA}), on the surface coverage with the poisonous adsorbate during the first 15 s at a constant electrode potential (E_{ad} = 0.2 V) is illustrated by CVs in Fig. 2. The respective CVs after various adsorption times at constant c_{FA}, which allow determination of the rate of the electrode coverage with FA residues ($d\theta/dt$), are shown in Fig. 3.

There is a general agreement that the strongly bound adsorbate is generated on a Pt electrode via the dissociative chemisorption of FA. Several possible CO-like surface species of various monomeric and dimeric structures (CO, HCO, COH, C_2O_3, $H_2C_2O_3$, HC_2O_3, HC_2O), coexisting in equilibrium on a Pt surface, were identified [59–70] depending on experimental conditions determined by various applied experimental techniques. Taking into account the obtained n_{eps} values (electrons per Pt site) of 1.6–2 and the fact that

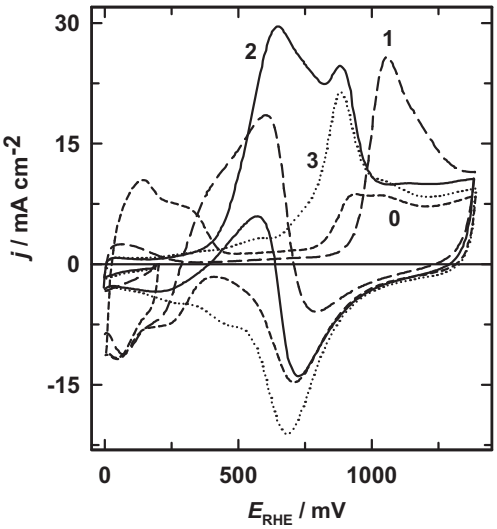

Fig. 1. CVs of a polycrystalline platinum electrode in solutions of 0.2 M $HClO_4$ (0), 0.2 M $HClO_4$ + 0.01 M FA (1), 0.2 M $HClO_4$ + 1 mM $Pb(ClO_4)_2$ + 0.01 M FA (2), 0.2 M $HClO_4$ + 1 mM $Pb(ClO_4)_2$ (3); dE/dt = 5 V s^{-1}, E_{ad} = 0.2 V, t_{ad} = 180 s.

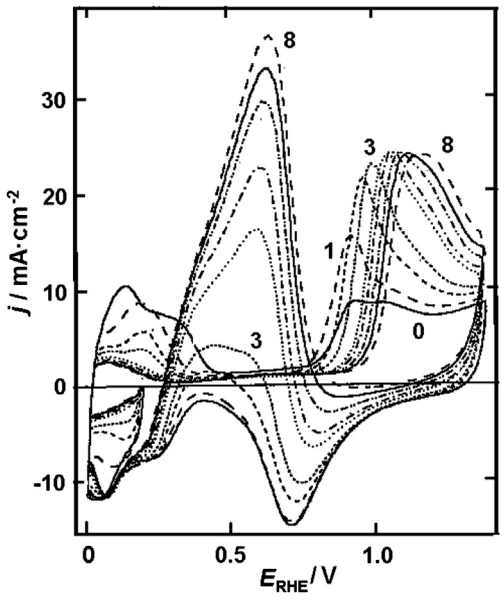

Fig. 2. CVs of a polycrystalline platinum electrode after t_{ad} = 15 s at E_{ad} = 0.2 V in solutions of 0.2 M $HClO_4$ (0), 0.2 M $HClO_4$ + 0.001 M FA (1), +0.005 M FA (2), +0.01 M FA (3), +0.05 M FA (4), +0.1 M FA (5), +0.25 M FA (6), +0.5 M FA (7), +1 M FA (8); dE/dt = 5 V s^{-1}.

oxidation of the FA adsorbate to CO_2 requires an electrode potential of 0.75 V or higher (see Figs. 2 and 3), the assumed existence of dimeric moieties besides the linearly- and bridge-bonded CO seems to be plausible. Some shift of the oxidative desorption of the FA residues toward more positive potentials at higher c_{FA} values and longer t_{ad} is undoubtedly connected to more difficult co-adsorption of oxygen-containing species indispensable for the occurrence of this reaction.

In accordance with the preliminary results reported previously for a Pt(100) electrode [4], a series of adsorption experiments performed in this work at various E_{ad} revealed that the rate of dissociative chemisorption of FA attains a maximum in the potential range around 0.2 V, i.e. close to zero charge potential of Pt ($E_{pzc,Pt}$ = 0.2 V [71]), at relatively low surface concentration of electrosorbed hydrogen ad-atoms. This suggests a specific orientation of the reactant at the Pt/solution interface as a precondition of the dissociative transformation of FA to CO_{ad}, being different from that of the FA species which undergo direct oxidation to CO_2 at $E > 0.4$ V (see Scheme 1).

Contrary to the situation on bare platinum, the dissociative chemisorption of FA accompanied by formation of strongly adsorbed residues becomes almost entirely suppressed on the Pt surface modified by underpotential deposition of Pb (upd-Pb). Simultaneously, the Pt/Pb electrode shows an excellent catalytic activity towards direct FA oxidation to CO_2 (identified by DEMS [72,73]). This phenomenon can always be observed at the concentration ratio of FA to Pb^{2+} cations in solution (trace 2 in Fig. 1) sufficient enough to ensure an almost complete coverage of Pt surface with Pb ad-atoms, before any surface reaction of FA can start. On a polycrystalline Pt electrode as used here we have found that the underpotential deposition of lead at a Pb^{2+} concentration of 10^{-3} M in acidic solution proceeds by about two orders of magnitude faster than the adsorption of strongly bonded FA moieties, even if the electrolyte solution contains a fifty-fold higher concentration of FA (0.05 M). It should be noted that the same regularity had been found by us on the Pt(100) electrode [4]. Consequently, under the above-mentioned experimental conditions there are no free Pt sites available for the dissociative chemisorption of FA which would result in poisoning of the Pt surface for further direct FA oxidation. The absence of irreversibly bonded residues of FA on the Pt/Pb surface can be understood in terms of the "third body" effect [74]. However, this effect alone cannot account for the efficient enhancement of the direct dehydrogenation of FA to CO_2 in comparison with bare Pt because the highest electrocatalytic activity of a Pt/Pb electrode is observed always at $\theta_{Pb} \approx 1$, whereas the formation of strongly adsorbed CO-like species from FA is already suppressed at $\theta_{Pb} < 0.5$ [4].

As depicted in the CVs in Fig. 1, the direct oxidation of FA to CO_2 on a Pt/Pb electrode is manifested as the current peak (2) with a maximum at 0.5–0.75 V (depending on c_{FA} and the scan rate). It is followed by the oxidative stripping of the upd Pb ad-layer; consequently the CV at $E > 0.9$ V displays features typical of the oxide formation on a blank Pt surface in the supporting electrolyte solution. This is convincing evidence for the absence of any strongly bound adsorbate on the surface of a Pt/Pb electrode and thus for inhibition of the dissociative chemisorption of FA within the potential range of hydrogen adsorption/desorption on Pt ($E \leq 0.4$ V). Additional support for this conclusion follows from the current density–time (j–t) transients obtained at various constant electrode potentials (E_{ad}) between 0.07 V and 0.2 V, which up to the FA concentration of about 0.05 M at a Pb^{2+} concentration of 10^{-3} M almost coincide with that obtained in the electrolyte solution containing lead cations alone (Fig. 4). This means that the cathodic charge transfer is related to the electroreduction of Pb^{2+} cations only. Already within the first 0.5 s after setting E_{ad} fast competitive coverage of the Pt surface with Pb ad-atoms brings about inhibition of dissociative chemisorption of FA on still vacant Pt sites and no

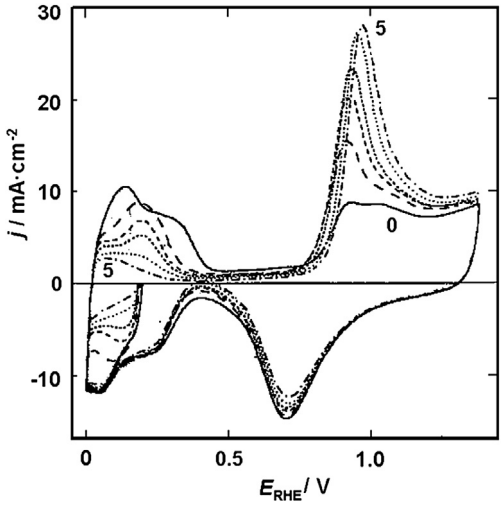

Fig. 3. CVs of a polycrystalline platinum electrode in solutions of 0.2 M $HClO_4$ (0), 0.2 M $HClO_4$ + 0.001 M FA (1–5) after adsorption at E_{ad} = 0.2 V for t_{ad} = 15 s (0, 1), 30 s (2), 60 s (3), 180 s (4), 900 s (5); dE/dt = 5 V s^{-1}.

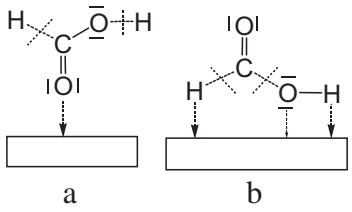

Scheme 1. Scheme of FA adsorbate a) on the upd-Pb-modified and unmodified platinum surfaces in the double layer region and b) on a bare Pt electrode in the hydrogen adsorption/desorption region.

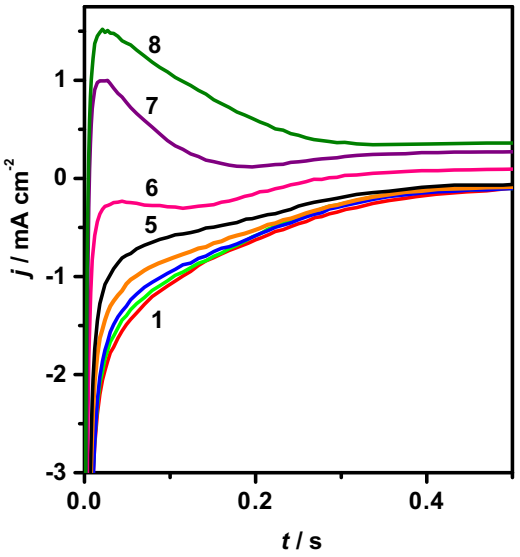

Fig. 4. Chronoamperograms of a polycrystalline platinum electrode at $E_{ad} = 0.2$ V in solutions of 0.2 M $HClO_4$ + 1 mM $Pb(ClO_4)_2$ (1), +0.001 M FA (2), +0.01 M FA (3), +0.05 M FA (4), +0.1 M FA (5), +0.25 M FA (6), +0.5 M FA (7), +1 M FA (8).

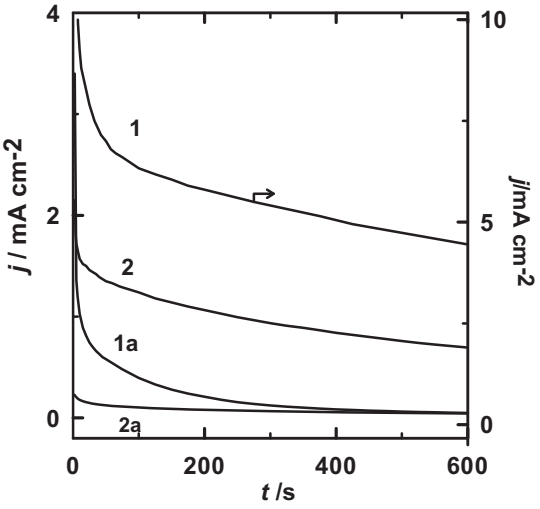

Fig. 5. Chronoamperograms (long term) of a polycrystalline platinum electrode in solutions of 0.2 M $HClO_4$ + 0.5 M FA at $E_{ad} = 0.4$ V (1a) and $E_{ad} = 0.3$ V (2a), and at Pt/Pb at $E_{ad} = 0.4$ V (1) and $E_{ad} = 0.3$ V (2).

further irreversibly bound FA species can be formed on the electrode surface. It is evident from j–t transients in Fig. 4, that upd-lead even at relatively high FA concentration $c_{FA} > 0.1$ M in the presence of 10^{-3} M Pb^{2+} in solution appears to be dominantly adsorbed on Pt. On the contrary, as shown above, the unmodified Pt electrode would be quickly poisoned with strongly bonded CO-like species in the absence of Pb^{2+} ions in a solution containing FA.

The conclusion, that the presence of FA in solution does not affect the rate of the Pt coverage with Pb ad-atoms up to the above mentioned concentration ratio $c_{FA}/c_{Pb^{2+}} \leq 50$ is – among others – confirmed by almost identical magnitudes of the Pb stripping peak current (with maximum around 0.9 V) obtained for the Pb^{2+}-containing electrolyte solution both with and without FA (see Fig. 1, traces 2 and 3). However, the anodic peak with a maximum around 1 V corresponding to oxidation of poisoning species would appear in CVs besides the stripping peak of the Pb ad-layer when at low $c_{Pb^{2+}}$ (for example $5 \cdot 10^{-5}$ M) the rates of formation of the Pb ad-layer and of FA dissociative chemisorption are similar or the rate of the latter reaction is higher. This observation corresponds well to the previously presented data on the strong competitive adsorption of upd-Pb ad-atoms and formaldehyde chemisorption [7].

If the dissociative chemisorption of FA resulting in formation of CO-like species is prevented due to the coverage of Pt surface sites with Pb, the direct oxidation of FA to CO_2 appears to be the only process occurring on a Pt/Pb electrode. Consequently, as shown in Fig. 5, the current density related to the FA oxidation during the long term transients at constant electrode potentials within the double layer range is markedly larger on a Pt electrode modified with Pb than on a bare Pt electrode, although the Pt/Pb electrode gets slightly poisoned with CO-like species at $c_{FA} \geq 0.1$ M in the electrolyte solution with $c_{Pb^{2+}} = 10^{-3}$ M. Obviously, the poisoning effect manifested as a moderate current decay with time can be easily minimized by increasing the concentration of Pb^{2+} up to 10^{-2} M or more, thus improving the rate of lead electrodeposition in competition to dissociative chemisorption of FA.

There is no doubt that modification of Pt surface with Pb ad-atoms causes a remarkable change in the adsorption properties of the electrode surface. The CVs in Fig. 6 reveal that a physisorbed precursor state including weakened bonds in the substrate molecules (see below) is formed on a Pt/Pb electrode as a precondition for the occurrence of a direct FA oxidation, which in the presence of 10^{-3} M Pb^{2+} in the supporting electrolyte solution starts already around $E \approx 0.1$ V at $c_{FA} \geq 0.1$ M. An increase in the current densities within the whole range of the respective anodic peak current on increasing the adsorption time (t_{ad}) at a fixed potential ($E_{ad} = 0.07$–0.2 V), prior to the first positive going sweep, indicates that the surface concentration of presumably physisorbed FA at the Pt/Pb electrode must be significantly increased. This conclusion is supported by the fact that the amount of FA accumulated at the

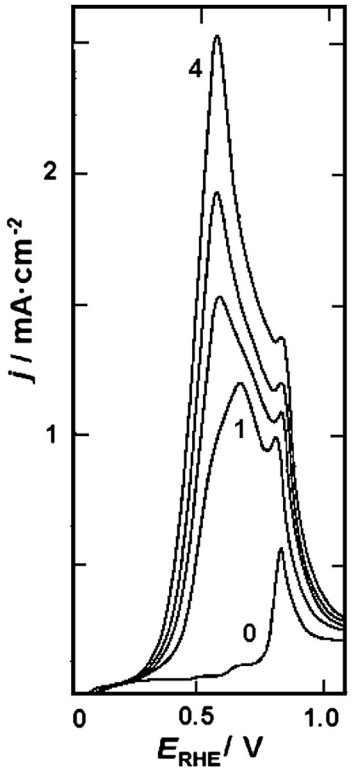

Fig. 6. CVs of a polycrystalline platinum electrode in solutions of 0.2 M $HClO_4$ + 1 mM $Pb(ClO_4)_2$ (0) + 5 mM FA after adsorption at $E_{ad} = 0.070$ V for $t_{ad} = 0$ s (0, 1), 30 s (2), 60 s (3), 180 s (4); $dE/dt = 0.1$ V s^{-1}.

electrode surface decreases successively in the following scans. Even at $dE/dt = 0.1$ V s^{-1} the time period of a potential cycle appears to be too short for renewed additional adsorption and appropriate transformation of bulk FA. As expected, the rate of FA physisorption and in consequence the current peak related to its direct oxidation to CO_2 become higher with increasing concentration of formic acid in solution. It is noteworthy that the presence of physisorbed FA at the electrode/solution interface was observed also when a bare Pt was applied as a catalyst of FA electrooxidation in the absence of Pb^{2+} ions in the electrolyte solution. However, the direct oxidation of physisorbed FA to CO_2 on an unmodified Pt electrode becomes visible in CVs (within the potential range of double layer) not until the oxidative desorption of strongly bonded CO-like species was completed during the first positive going sweep, at $E > 0.9$ V (Fig. 7). Moreover, this process occurs in parallel to the dissociative chemisorption and the amount of physisorbed FA at a Pt/solution interface is much smaller than that at the Pt/Pb electrode.

Further information about the transition state and the rate determining step (rds) in the FA oxidation on the Pt/Pb electrode can be gained from experiments with deuterium labelled compounds [75–79]. In our previous studies, the kinetic isotope effect was successfully used to obtain mechanistic details related to the main reaction steps in the electrooxidation of formaldehyde on Pt [7] and of aliphatic alcohols on gold [80,81].

The influence of the systematic H/D substitution on the kinetics of FA oxidation to CO_2 on a Pt electrode modified with upd-Pb and free of poisoning species under the chosen experimental conditions is clearly visible in CVs exemplified in Fig. 8. The rate of the investigated process gradually decreases with increasing extent of the H/D exchange, whereas Tafel plots show the same slope ($dE/d\log j = 90 \pm 5$ mV dec^{-1}) for various concentrations of unlabelled and deuterated compounds.

Comparison of the current densities related to electrooxidation of HCOOH, DCOOH and DCOOD on a Pt/Pb electrode in the kinetic region of CVs (wherein the Tafel evaluation was performed) yields:

$$j_{H_2O}^{HCOOH}/j_{H_2O}^{DCOOH} = 3 \pm 0.1, \quad j_{H_2O}^{DCOOH}/j_{D_2O}^{DCOOD} = 2.8 \pm 0.1 \quad j_{H_2O}^{HCOOH}/j_{D_2O}^{DCOOD} = 8.5 \pm 0.1$$

The oxidation rate of DCOOH, after substitution of hydrogen in the C–H bond with deuterium, is diminished to 1/3 of that characteristic of HCOOH at the same concentration. With the completely deuterated DCOOD in the deuterated electrolyte solution, the reaction rate decreases by a factor of 8.5. This means a 2.8-fold decrease in the current due to substitution of deuterium in the OH group. These changes in the oxidation current, indicating a primary kinetic isotope effect, comparable to that calculated for catalytic decomposition of gaseous FA in a chemical reactor [82], are additionally illustrated in Fig. 9 showing oxidation currents as a function of the FA concentration in solution. Since the degree of H/D substitution does not influence the Tafel slopes and the reaction

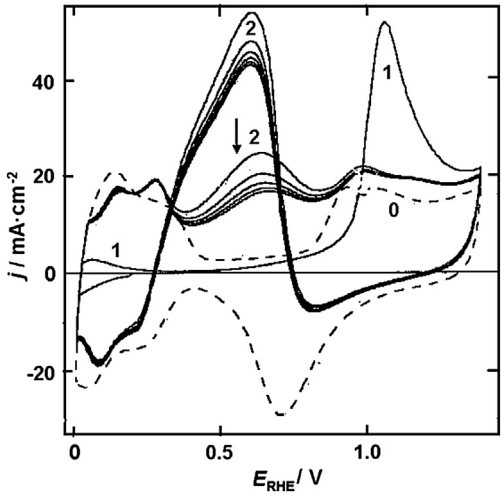

Fig. 7. CVs of a polycrystalline platinum electrode in a solution of 0.2 M $HClO_4$ (0) + 0.1 M FA after adsorption at $E_{ad} = 0.2$ V for $t_{ad} = 180$ s (1: first cycle, 2: second and following cycles); $dE/dt = 10$ V s^{-1}.

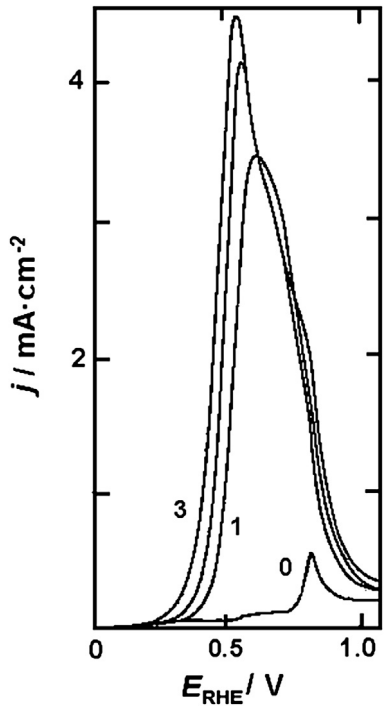

Fig. 8. CVs of a polycrystalline platinum electrode in solutions of 1 mM $Pb(ClO_4)_2$ (0) + 0.01 M DCOOD/D_2O (1), DCOOH/H_2O (2), HCOOH/H_2O (3); (1) with 0.2 M $DClO_4$; (0) (2,3) with 0.2 M $HClO_4$; $dE/dt = 0.1$ V s^{-1}.

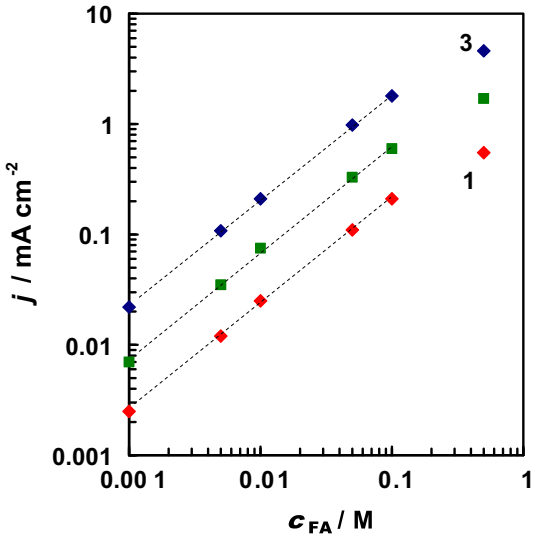

Fig. 9. Plot of electrooxidation current as a function of FA concentration after $t_{ad} = 180$ s at $E_{ad} = 0.2$ V at $E_{ox} = 0.36$ V for Pt electrode in solutions of: 1 mM $Pb(ClO_4)_2$ + DCOOD/D_2O (1); DCOOH/H_2O (2); HCOOH/H_2O (3); (1) with 0.2 M $DClO_4$; (2, 3) with 0.2 M $HClO_4$; after $t_{ad} = 180$ s at $E_{ad} = 0.2$ V.

order with respect to the substrate equals $z_{FA} = 1$ up to an FA concentration of 0.05 M, the same reaction mechanism should be operative for undeuterated and deuterated compounds. It should be noted that analysis of long term chronoamperometric data obtained on a Pt/Pb electrode at various constant potentials from the Tafel range revealed the same differences in the oxidation rate of unlabelled FA and its deuterated derivates as those resulting from CVs. Interestingly, a similar effect of deuterium substitution in C–H and O–H bonds on the rate of the direct FA oxidation to CO_2 was found also on a freshly activated Pt electrode in the absence of Pb^{2+} ions when the initial part of CVs was analysed upon the first positive going sweep (at $v \geq 0.1$V s^{-1}), immediately after switching ($v = 10$ V s^{-1}) from 1.5 V to the starting electrode potential between 0.07 V and 0.2 V. The absence of strongly adsorbed moieties on the Pt surface under such conditions was clearly evidenced by the lack of any suppression of hydrogen adsorption states (data will be presented elsewhere).

Almost the same primary kinetic isotope effect for deuterium substitution at the carbon and the oxygen atoms observed on a Pt/Pb electrode as well as on a Pt electrode free of strongly adsorbed CO-like species support the view that simultaneous cleavage of the C–H/C–D and O–H/O–D bonds is involved in the rds of the direct electrooxidation of FA to CO_2. Most probably these bonds are both weakened to a similar extent in a transition state formed at the electrode/solution interface under the influence of the electrode potential. As a consequence, two electrons may be transferred to the electrode at a similar rate, almost simultaneously.

The possible types of adsorbed transition complexes of FA on the Pt/Pb and bare Pt electrode surface in the double layer region interacting through the carbonyl group or through both hydrogen atoms on Pt in the hydrogen adsorption/desorption range are depicted in Scheme 1. The former orientation of FA molecules (Scheme 1a) seems to be likely for the direct oxidation to CO_2 since this reaction occurs on a positively charged Pt/Pb electrode ($E_{pzc,Pb} = -0.7$ V [83]). This is also valid for the direct oxidation of FA to CO_2 on the Pt electrode with $E_{pzc,Pt} = 0.2$ V [71]. Obviously, an inductive effect connected with such an interaction may contribute to the loosening of both the C–H- and O–H-bonds enabling the release of two hydrogen atoms and one electron in the first charge-transfer step:

$$HCOOH_{ad} \rightarrow {}_xCOO^- + 2H^+ + e^-$$

and yielding CO_2 in the second charge-transfer step:

$${}_xCOO^- \rightarrow CO_2 + e^-$$

The above mechanism involving a simultaneous release of two hydrogen atoms differs from the previously suggested one, wherein the C–H- and O–H-bonds were split in two successive charge transfer steps, with adsorbed $COOH_{ad}$ [60,84] or bridge-bonded formate ($HCOO_{ad}$) species [61–70] as possible intermediates. The presence of the latter species on the Pt surface in the potential range between 0.2 V and 0.6 V was suggested on the basis of the observation of a weak band at about 1300 cm^{-1} attributed to the symmetrical stretching vibrations of COO group, besides the bands at 1790–1880 cm^{-1} and 2000–2080 cm^{-1} assigned to the linearly- and multifold-bonded CO_{ad} species in the *in situ* IR spectra [60–67]. However, this interpretation appears to be disputable because the band typical of asymmetrical stretching vibrations of the carboxylate group at about 1600 cm^{-1} (see Refs. [85,86]) was not observed in these spectra. Moreover, since FA labelled with deuterium at the C atom only was used in earlier studies of the direct FA oxidation to CO_2 [64], the primary kinetic isotope effect connected with O–H/O–D bond cleavage remained undetected, although the kinetic effect observed in Ref. [64] upon H/D substitution at the carbon atom and that obtained in the present paper are in full agreement.

The alternative FA adsorbate (Scheme 1b) formed at Pt surface sites, mostly in the hydrogen adsorption-desorption region, is conducive to water release and generation of the poisoning CO_{ad} species. Accordingly, a secondary kinetic isotope effect was derived from a comparison of the CVs obtained after setting a constant value of E_{ad} (between 0.07 V and 0.2 V) on the Pt electrode in electrolyte solution containing DCOOH (Fig. 10) or HCOOH (Fig. 3). The rate of dissociative chemisorption of FA, deduced from the coverage of the Pt surface (θ) with irreversibly bound adsorbate as a function of adsorption time (kinetic adsorption isotherms) was decreased by a factor of 1.5–2 on substitution of deuterium in the C–H bond. In parallel, insignificant differences in the θ values were observed between DCOOH and DCOOD for $c_{FA} = \text{const.}$ at a given t_{ad}. The same phenomenon was observed in the j–t transients measured at E_{ad} within the above mentioned potential range on Pt as well as on Pt/Pb electrodes when the rate of underpotential Pb deposition under such conditions was insufficient to avoid the adsorption of strongly bonded FA residues formed during dissociative chemisorption of this compound on still free Pt sites. According to theoretical calculations [77,82] the secondary kinetic isotope with a factor of 1.5–2 between HCOOH and DCOOH observed with a platinum electrode might suggest the oxidative desorption of hydrogen, resulting from the cleavage of the C–H/C–D bond in FA as the rate determining step. Furthermore, as follows from the very similar behaviour of DCOOH and DCOOD, the C–OH and not O–H bond breaks in the dissociative chemisorption of FA on Pt surface sites. The question remains open about the sequence of the reaction steps, i.e. if C–H bond is broken in the first step of the FA dehydration to CO_{ad} or both C–H and C–OH bonds are split simultaneously. However, there is no doubt that the removal of OH group from the FA molecule via a reaction with hydrogen ad-atoms present on the adjacent Pt sites can be excluded. This conclusion is justified by a much lower rate of poisoning of the Pt electrode at $E = 0.07$ V in comparison to that at $E = 0.2$ V, although the surface concentration of hydrogen ad-atoms is higher at the former potential. A similar opinion has been presented also by other authors for various monocrystalline Pt electrodes [68].

It should be borne in mind that a lead electrode is inactive for the oxidative dehydrogenation of FA, whereas a coverage of upd-lead ad-atoms on Pt not only prevents the formation of strongly adsorbed poisoning species (being the dominant process on bare Pt

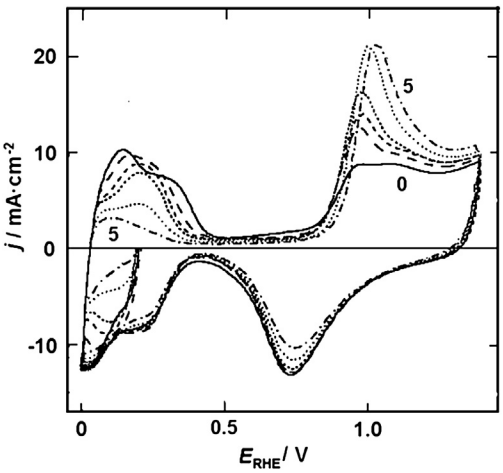

Fig. 10. CVs of a polycrystalline platinum electrode in solutions of 0.2 M $HClO_4$ + 0.001 M DCOOH/H_2O (0) and after adsorption at $E_{ad} = 0.2$ V for $t_{ad} = 15$ s (1), 30 s (2), 60 s (3), 180 (4), 600 s (5); $dE/dt = 5$ V s^{-1}.

at $E \leq 0.4$ V) but also shows a pronounced synergistic effect in the direct FA electrooxidation to CO_2. Thus, taking into account the results presented above, it seems reasonable to assume that the enhanced catalytic activity of Pt/Pb electrode is a consequence of the modification of the electronic band structure of the surface Pb-atoms due to their interactions with the Pt-atoms underneath. This changes the adsorptive properties of the Pt/Pb surface as compared with those of Pb and Pt, contributing both to inhibition of formation of poisoning species and to the synergetic effect in electrocatalytic dehydrogenation of FA resulting in evolution of CO_2. Changes in the value of E_{pzc} (a more negative value for lead than for platinum [71,83]) may in addition influence the reactant orientation at the electrode/solution interface and thus the kinetics and the reaction products of the process investigated.

4. Conclusions

Results of kinetic and mechanistic studies of formic acid oxidation on a bare platinum and a lead ad-atoms covered platinum electrode using unlabelled and deuterated compounds provided clear evidence that poisoning of the Pt surface sites with strongly bonded species can be prevented by suppression of dissociative chemisorption of FA due to a fast competitive underpotential deposition of lead ad-atoms. Modification of Pt surface with upd-lead induces a catalytic synergistic effect in the direct oxidation of physisorbed FA molecules to CO_2. From the observed kinetic isotope effect it follows that the simultaneous cleavage of C–H/C–D and O–H/O–D bonds is involved in the rds of this process. On the other hand, it is the C–OH bond and not the O–H one that splits in the dissociative chemisorption of FA on Pt surface sites which involves elimination of water molecule and generation of poisoning CO-like species. The optimal conditions for monitoring of FA in acidic solution containing Pb^{2+} cations were specified.

Acknowledgements

Financial support by the Ministry of Science, Poland, and a travel grant by the Alexander von Humboldt-Stiftung to one of us (R.H.) are gratefully acknowledged.

References

[1] M.M.P. Janssen, J. Molhuysen, Electrochim. Acta 21 (1976) 869–878.
[2] D. Pletcher, V. Solis, J. Electroanal. Chem. 131 (1982) 309–323.
[3] M. Shabrang, H. Mizota, S. Bruckenstein, J. Electrochem. Soc. 131 (1984) 306–314.
[4] M. Bełtowska-Brzezinska, J. Heitbaum, W. Vielstich, Electrochim. Acta 30 (1985) 1465–1471.
[5] A.A. El-Shafei, S.A. Abd El-Maksoud, M.N.H. Moussa, J. Electroanal. Chem. 336 (1992) 73–83.
[6] A.A. El-Shafei, H.M. Shabanah, M.N.H. Moussa, J. Electroanal. Chem. 362 (1993) 159–165.
[7] M. Bełtowska-Brzezinska, J. Stelmach, Z. Physiol. Chem. 185 (1994) 91–102.
[8] M. Krausa, W. Vielstich, J. Electroanal. Chem. 379 (1994) 307–314.
[9] K.A. Friedrich, K.P. Geyzers, U. Linke, U. Stimming, J. Stumper, J. Electroanal. Chem. 402 (1996) 123–128.
[10] W. Chrzanowski, A. Wieckowski, Langmuir 14 (1998) 1967–1970.
[11] H. Wang, Ch. Wingender, H. Baltruschat, M. Lopez, M.T. Reetz, J. Electroanal. Chem. 509 (2001) 163–169.
[12] E. Gyenge, in: J. Zhang (Ed.), PEM Fuel Cell Electrocatalysts and Catalyst Layers; Fundamentals and Applications, Springer Verlag, London, 2008, pp. 164–285.
[13] F.J. Vidal-Iglesias, J. Solla-Gullón, E. Herrero, A. Aldaz, J.M. Feliu, J. Appl. Electrochem. 36 (2006) 1207–1214.
[14] V. Del-Colle, A. Berna, G. Tremiliosi-Filho, E. Herrero, J.M. Feliu, Phys. Chem. Chem. Phys. 10 (2008) 3766–3773.
[15] M.D. Obradović, A.V. Tripković, L. Snezana, J. Gojković, Electrochim. Acta 55 (2009) 204–209.
[16] J. Souza-Garcia, E. Herrero, J.M. Feliu, Chem. Phys. Chem. 11 (2010) 1391–1394.
[17] Q.-S. Chen, Z.-Y. Zhou, F.J. Vidal-Iglesias, J. Solla-Gullon, J.M. Feliu, S.-G. Sun, J. Am. Chem. Soc. 133 (2011) 12930–12933.
[18] E. Mostafa, A. El-Aziz, A. Abd-El-Latif, R. Ilsley, G. Attardd, H. Baltruschat, Phys. Chem. Chem. Phys. 14 (2012) 16115–16129.
[19] M. Bełtowska-Brzezinska, J. Heitbaum, J. Electroanal. Chem. 183 (1985) 167–181.
[20] J. Stelmach, R. Holze, M. Bełtowska-Brzezinska, J. Electroanal. Chem. 377 (1994) 241–247.
[21] N. Markowic, H. Gasteiger, A. Ross, P.N. Villegas, M.J. Weaver, Electrochim. Acta 40 (1995) 91–98.
[22] H. Hoster, T. Iwasita, H. Baumgartner, W. Vielstich, Phys. Chem. Chem. Phys. 3 (2001) 337–346.
[23] U.B. Demirci, J. Power Sources 173 (2007) 11–18.
[24] S. Park, Y. Xie, M.J. Weaver, Langmuir 18 (2002) 5792–5798.
[25] A. Wieckowski, E.R. Savinova, C.G. Vavenas (Eds.), Catalysis and Electrocatalysis at Nanoparticle Surfaces, Marcel Dekker Inc., New York, 2003, pp. 1–960.
[26] J.D. Lovic, A.V. Tripkovic, J. Gojkovic, K.D. Popovic, D.V. Tripkovic, P. Olszewski, A. Kowal, J. Electroanal. Chem. 581 (2005) 294–302.
[27] R.R. Adzic, J. Zhang, K. Sasaki, M.B. Vukmirovic, M. Shao, J.X. Wang, A.U. Nilekar, M. Mavrikakis, J.A. Valerio, F. Uribe, Top. Catal. 46 (2007) 249–262.
[28] J. Zhang, P. Liu, H. Ma, Y. Ding, J. Phys. Chem. C 111 (2007) 10382–10388.
[29] H.I. Lee, S.E. Habas, G.A. Somorjai, P.D. Yang, J. Am. Chem. Soc. 130 (2008) 5406–5407.
[30] S. Guo, E. Wang, Anal. Chim. Acta 598 (2007) 181–192.
[31] M. Schrinner, S. Proch, Y. Mei, R. Kempe, N. Miyajima, M. Ballauff, Adv. Mater. 20 (2008) 1928–1933.
[32] F. Maillard, S. Pronkin, E.R. Savinova, in: W. Vielstich, H.A. Gasteiger, H. Yokokawa (Eds.), Handbook of Fuel Cells, Advances in Electrocatalysis, Materials, Diagnostics and Durability, vol. 5, John Wiley & Sons Inc., New York, 2009, pp. 91–111.
[33] A. Maljusch, T.C. Nagaiah, S. Schwamborn, M. Bron, W. Schuhmann, Anal. Chem. 82 (2010) 1890–1896.
[34] K.R. Beyerlein, J. Solla-Gullón, E. Herrero, E. Garnier, F. Pailloux, M. Leoni, P. Scardi, R.L. Snyder, A. Aldaz, J.M. Feliu, Mater. Sci. Eng. A 528 (2010) 83–90.
[35] F.J. Vidal-Iglesias, J. Solla-Gullón, E. Herrero, A. Aldaz, J.M. Feliu, Angew. Chem. Int. Ed. 49 (2010) 6998–7001.
[36] S.A. Mamuru, K.I. Ozoemena, T. Fukuda, N. Kobayashi, J. Mater. Chem. 20 (2010) 10705–10715.
[37] M.N. Wanjala, J. Luo, B. Fang, D. Mott, C.-J. Zhong, J. Mater. Chem. 21 (2011) 4012–4020.
[38] S. Żołądek, I.A. Rutkowska, K. Skorupska, B. Palys, P.J. Kulesza, Electrochim. Acta 56 (2011) 10744–10750.
[39] C.-H. Cui, J.-W. Yu, H.-H. Li, M.-R. Gao, H.-W. Liang, S.-H. Yu, ACS Nano 5 (2011) 4211–4218.
[40] J. Seweryn, A. Lewera, J. Power Sources 205 (2012) 264–271.
[41] M. Li, W.-P. Zhou, N.S. Marinkovic, K. Sasaki, R.R. Adzic, Electrochim. Acta 104 (2013) 454–461.
[42] P.-C. Su, H.-S. Chen, T.-Y. Chen, C.-W. Liu, C.-H. Lee, J.-F. Lee, T.-S. Chan, K.-W. Wang, Int. J. Hydrogen Energy 38 (2013) 4474–4482.
[43] C. D'Urso, A. Bonesi, W.E. Triaca, A.M. Castro Luna, V. Baglio, A.S. Arico, Int. J. Electrochem. Sci. 7 (2012) 9909–9919.
[44] S. Zhang, S. Guo, H. Zhu, D. Su, S. Sun, J. Am. Chem. Soc. 134 (2012) 5060–5063.
[45] A. Bonnefont, A.N. Simonov, S.N. Pronkin, E.Y. Gerasimov, P.A. Pyrjaev, V.N. Parmon, E.R. Savinova, Catal. Today 202 (2013) 70–78.
[46] R.B. Moghaddam, P.G. Pickup, Electrochim. Acta 65 (2012) 210–215.
[47] M. Cargnello, N.L. Wieder, T. Montini, R.J. Gorte, P. Fornasiero, J. Am. Chem. Soc. 132 (2010) 1402–1409.
[48] A.J. Wain, Electrochim. Acta 92 (2013) 383–391.
[49] M.-Y. Duan, R. Liang, N. Tian, Y.-J. Lia, E.S. Yeung, Electrochim. Acta 87 (2013) 432–437.
[50] S. Yang, H. Lee, ACS Catal. 3 (2013) 437–443.
[51] M.E. Leunissen, C.G. Christova, A.P. Hynninen, C.P. Royall, A.L. Campbell, A. Imhof, M. Dijkstra, R. VanRoij, A. VanBlaaderen, Nature 437 (2005) 235–240.
[52] B. Ballarin, M.C. Cassani, E. Scavetta, D. Tonelli, Electrochim. Acta 53 (2008) 8034–8044.
[53] P. Arunkumar, S. Berchmans, V. Yegnaraman, J. Phys. Chem. C 113 (2009) 8378–8386.
[54] S. Berchmans, P. Arunkumar, S. Lalitha, V. Yegnaraman, Ber. Appl. Catal. B 88 (2009) 557–563.
[55] S. Zhang, Y. Shao, G. Yin, Y. Lin, Angew. Chem. Int. Ed. 49 (2010) 2211–2214.
[56] K. Barman, S. Jasimuddin, Ind. J. Chem. A 52 (2013) 217–220.
[57] F.G. Will, H.J. Hess, J. Electrochem. Soc. 133 (1986) 454–455.
[58] T. Biegler, D.A.J. Rand, R. Woods, J. Electroanal. Chem. 29 (1971) 269–277.
[59] B. Folkesson, R. Larson, J. Zander, J. Electroanal. Chem. 267 (1989) 149–161.
[60] R. Parsons, T. VanderNoot, J. Electroanal. Chem. 257 (1988) 9–45.
[61] A. Miki, S. Ye, M. Osawa, Chem. Commun. (2002) 1500–1501.
[62] G. Samjeske, A. Miki, S. Ye, M. Osawa, J. Phys. Chem. B 110 (2006) 16559–16566.
[63] Y.-X. Chen, S. Ye, M. Heinen, Z. Jusys, M. Osawa, R.J. Behm, J. Phys. Chem. B 110 (2006) 9534–9544.
[64] Y.-X. Chen, M. Heinen, Z. Jusys, R.J. Behm, Chem. Phys. Chem. 8 (2007) 380–385.
[65] M. Osawa, K.-I. Komatsu, G. Samjeske, T. Uchida, T. Ikeshoji, A. Cuesta, C. Gutierrez, Angew. Chem. Int. Ed. 50 (2011) 1159–1163.
[66] A. Cuesta, G. Cabello, C. Gutiérrez, M. Osawa, Phys. Chem. Chem. Phys. 13 (2011) 20091–20095.
[67] A. Cuesta, G. Cabello, M. Osawa, C. Gutiérrez, ACS Catal. 2 (2012) 728–738.
[68] V. Grozovski, V. Climet, E. Herrero, J.M. Feliu, Chem. Phys. Chem. 10 (2009) 1922–1926.
[69] V. Grozovski, F.J. Vidal-Iglesias, E. Herrero, J.M. Feliu, Chem. Phys. Chem. 12 (2011) 1641–1644.

[70] M. Neurock, M. Janik, A. Wieckowski, Faraday Discuss. 140 (2009) 363–378.
[71] R. Holze, in: W. Martienssen, M.D. Lechner (Eds.), Landolt-Börnstein: Numerical Data and Functional Relationships in Science and Technology, New Series, Group IV: Physical Chemistry, Electrochemistry, Subvolume A: Electrochemical Thermodynamics and Kinetics, vol 9, Springer-Verlag, Berlin, 2007, p. 220.
[72] O. Wolter, J. Willsau, J. Heitbaum, J. Electrochem. Soc. 132 (1985) 1635–1638.
[73] N.A. Anastasijevic, H. Baltruschat, J. Heitbaum, J. Electroanal. Chem. 272 (1989) 89–100.
[74] H. Angerstein-Kozłowska, B. MacDougall, B.E. Conway, J. Electrochem. Soc. 120 (1973) 756–766.
[75] K.J. Laidler, Chemical Kinetics, Harper Collins, New York, 1987, p. 221.
[76] A. Jarczewski, Wiad. Chem. 28 (1974) 529–542.
[77] G. Schroeder, A. Jarczewski, A. Dorożalska, Wiad. Chem. 31 (1977) 293–301.
[78] A. Jarczewski, P. Pruszyński, Wiad. Chem. 32 (1978) 693–704.
[79] A. Jarczewski, C.D. Hubbard, J. Mol. Struct. 649 (2003) 287–307.
[80] M. Bełtowska-Brzezinska, W. Vielstich, Electrochim. Acta 22 (1977) 1313–1314.
[81] R. Holze, T. Łuczak, M. Bełtowska-Brzezinska, Electrochim. Acta 39 (1994) 485–489.
[82] J. Block, H. Kral, Z. Elektrochem. 63 (1959) 182–190.
[83] B.B. Damaskin, O.A. Petrii, V.V. Batrakov, Adsorption Organischer Verbindungen an Elektroden, Akademie-Verlag, Berlin, 1975.
[84] S.-G. Sun, J. Clavilier, A. Bewick, J. Electroanal. Chem. 240 (1988) 147–159.
[85] D.L. Pavia, G.M. Mampman, G.S. Kriz, in: J. Vondeling (Ed.), Introduction to Spectroscopy, Brooks/Cole Thomson Learning, USA, 2001.
[86] L.D. Field, S. Sternhell, J.R. Kalman, Organic Structures from Spectra, John Wiley and Sons, New York, 2007.